Journal of Photochemistry and Photobiology A: Chemistry 230 (2012) 55–64

Contents lists available at SciVerse ScienceDirect

Journal of Photochemistry and Photobiology A: Chemistry

journal homepage: www.elsevier.com/locate/jphotochem

Oligofluorene-based push–pull type functional materials for blue light-emitting diodes

Ying Lin[a,b], Yu Chen[a,*], Teng-Ling Ye[c], Zhi-Kuan Chen[b,*], Yan-Feng Dai[c], Dong-Ge Ma[c,*]

[a] Shanghai Key Laboratory of Functional Materials Chemistry, Institute of Applied Chemistry, East China University of Science and Technology, 130 Meilong Road, Shanghai 200237, China
[b] Institute of Materials Research and Engineering, 3 Research Link, Singapore 117602, Singapore
[c] State Key Laboratory of Polymer Physics and Chemistry, Changchun Institute of Applied Chemistry, Chinese Academy of Sciences, Graduate School of the Chinese Academy of Sciences, Changchun 130022, China

ARTICLE INFO

Article history:
Received 25 September 2011
Received in revised form 4 December 2011
Accepted 14 December 2011
Available online 24 December 2011

Keywords:
Oligofluorene
OLED
Cyanophenyl
Carbazole
Push–pull type functional materials

ABSTRACT

A series of new oligofluorene-based push–pull type blue light-emitting functional materials, namely, 2-(9*H*-carbazole-9-yl)-7-(4-cyanophenyl)-9,9-dihexylfluorene (**F1**), 7-(9*H*-carbazol-9-yl)-7′-(4-cyanophenyl)-2,2′-bi(9,9-dihexylfluorene) (**F2**), 7-(9*H*-carbazole-9-yl)-7″-(4-cyanophenyl)-2,2′:7′,2″-ter(9,9-dihexylfluorene) (**F3**), and 7-(9*H*-carbazole-9-yl)-7‴-(4-cyanophenyl)-2,2′:7′,2″:7″,2‴-quarter(9,9-dihexylfluorene) (**F4**) were synthesized and characterized. Their onset decomposition temperatures for the thermal bond cleavage and the glass-transition temperatures were in general increased with increasing number of fluorene units. In dilute toluene solution, the oligofluorenes exhibited main absorption peaks in the range of 343–370 nm, photoluminescence maxima from 403 to 410 nm, and absolute quantum yields (Φ_{PL}s) of higher than 87%. In contrast, the absorption spectra of these compounds in the thin films had no large differences from those in the solutions except for the slight peak red-shifts (2–8 nm). The main emission maxima of **F1**, **F2**, and **F3** in the thin films were located at 418–420 nm, while the main emission of **F4** was found to be shifted to 446 nm, followed by a shoulder peak at 421 nm. The Φ_{PL}s of these thin films were estimated in the range of 59.2–68.7%. The existence of the electron-pull and -push end groups could effectively tune the energy levels of the oligofluorenes. By using the organic light emitting device (OLED) configuration of ITO/PEDOT:PSS/oligofluorenes/TPBi/LiF/Al by solution-process, **F4** displayed the best performance: the lowest turn-on voltage (4.1 V) and highest maximum luminance (2180 cd/m^2) with maximal current efficiency of 1.17 cd/A. When **F4** was fabricated into the optimized device of ITO/MoO_3/NPB/CBP:**F4**(1:4)/TPBi/LiF/Al by vapor deposition, highest brightness of 5135 cd/m^2 and current efficiency of 1.76 cd/A were achieved with the Commission Internationale de l'Eclairage (CIE) coordinates of (0.16, 0.09).

1. Introduction

As very promising active functional materials, π-conjugated organic oligomers with high chemical purity and well-defined molecular structures have attracted considerable interest owing to their great potential for applications in organic thin film electronic devices such as organic light-emitting diodes (OLEDs) [1–3], organic photovoltaic (OPV) cells [4–6], and organic field effect transistors (OFETs) [7–9]. During the past 20 years, much progress has been made in the field of OLEDs that represent a promising technology for large, flexible, lightweight, flat-panel displays that could replace liquid-crystal displays or cathode-ray tubes. Compared to the well-established green- and red-emitting materials, stable and high-performance blue light-emitting materials and corresponding optimized device structures are still under development. Among the many reported organic oligomers used as the blue emitters, fluorene-based oligomers with two or three fluorenyl repeat units having different functional groups at the C-9 position of the fluorene unit have been used as a good blue light source and/or, as the host material that can be used to realize other color emissions, as a result of their excellent thermal stability, high fluorescent quantum yield, and outstanding electroluminescent behavior [10–14].

It is necessary to increase the injection and transport of the electrons and holes to produce more excitons in the active polymers. Many hole-transporting groups such as triarylamine and carbazole have been covalently incorporated into the oligofluorenes by a variety of reactions as part of the backbone, the end of side chain, branch points of star, and end-capping groups. For example, Ma et al. [15] reported the synthesis of spirobifluorene trimers with

* Corresponding authors.
E-mail addresses: chentangyu@yahoo.com (Y. Chen), zk-chen@imre.a-star.edu.sg (Z.-K. Chen), mdg1014@ciac.jl.cn (D.-G. Ma).

1010-6030/$ – see front matter © 2011 Elsevier B.V. All rights reserved.
doi:10.1016/j.jphotochem.2011.12.008

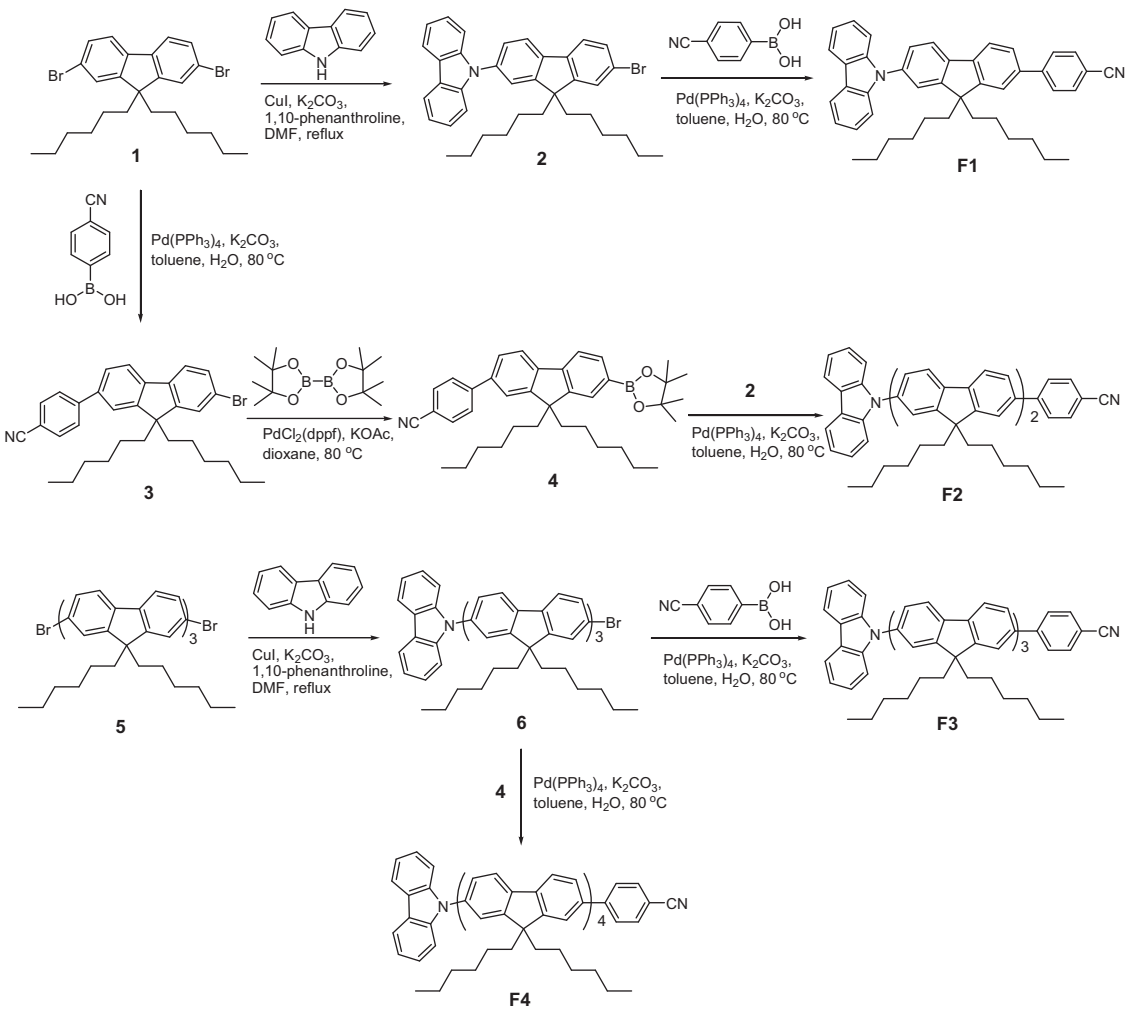

Scheme 1. Synthetic routes of **F1–F4**.

peripheral carbazole groups as side chains. These compounds have higher HOMO energy levels and better hole-injection abilities in comparison with the trimers without carbazoles. A series of multi-H shaped oligofluorenes surrounded by triphenylamine units through the C-9's of the central fluorene with pure blue electroluminescence and high HOMO energy levels were studied by Tao et al. [16]. Four starburst oligomers bearing a 4,4′,4″-tris(carbazol-9-yl)-triphenylamine (TCTA) core and six oligofluorene arms were also reported to demonstrate that the presence of the TCTA was crucial for the hole-transporting [17]. Using Ullmann coupling reaction, Promarak et al. [18] prepared a series of *N*-carbazole end-capped oligofluorenes with 1, 2, and 3 fluorene units and found that these molecules exhibited red shifts in absorption and photoluminescence spectra with respect to the number of fluorene units and excellent electrochemical reversibility. In such a system energy or exciton can efficiently transfer from the peripheral carbazole via the lone electron pair of the nitrogen atom to the oligofluorene backbone. Using either palladium catalyzed cross-coupling reaction or nickel-catalyzed reductive dimerization, the same authors designed and synthesized a series of new *N*-carbazole end-capped oligofluorene–thiophenes with one, two, three, and four thiophene rings [19]. The terminal carbazole and fluorene moieties of the resulting materials are beneficial for their morphology, conjugation length, and solubility. Although these carbazole end-capped oligomers were potential blue light-emitting materials with improved hole affinity, the corresponding OLED device performance was deficient. To address this problem, covalent grafting of electron-withdrawing and donating groups onto the two sides of the oligofluorene backbone, respectively, would be an effective way to improve the charge injection of blue light-emitting oligomers. In the family of electron deficient units such as cyano group [20–23], oxadiazole [24,25], quinoline [26,27], pyridine [28,29], and others, the cyano group has been demonstrated to possess prominent capacities of electron affinity and luminance [30,31]. For these reasons, we, for the first time, prepared a series of oligofluorenes end-capped by cyanophenyl and carbazole units: 2-(9*H*-carbazole-9-yl)-7-(4-cyanophenyl)-9,9-dihexyl- fluorene (**F1**), 7-(9*H*-carbazol-9-yl)-7′-(4-cyanophenyl)-2,2′-bi(9,9-dihexylfluorene) (**F2**), 7-(9*H*-carbazole-9-yl)-7″-(4-cyanophenyl)-2,2′:7′,2″-ter(9,9-dihexylfluorene) (**F3**), and 7-(9*H*-carbazole-9-yl)-7‴-(4-cyanophenyl)-2,2′:7′,2″:7″,2‴-quarter(9,9-dihexylfluorene) (**F4**), as shown in Scheme 1. As a result, when **F4** was fabricated into an optimized device of ITO/MoO_3/NPB/CBP:**F4**(1:4)/TPBi/LiF/Al by vapor deposition, highest brightness of 5135 cd/m^2 and current efficiency of 1.76 cd/A were achieved with the CIE coordinates of (0.16, 0.09).

2. Experimental

2.1. General

Organic solvents were purified, dried, and distilled under dry nitrogen. 2,7-dibromo-9,9-dihexylfluorene (**1**) was purchased from Sigma–Aldrich. 4-Cyanophenyl-boronic acid and

bis(pinacolato)diboron were bought from Boron Molecular. Copper(I) iodine and 1,10-phenanthroline were from Merck and Lancaster, respectively. Tetrakistriphenylphosphine palladium(0) [$Pd(PPh_3)_4$] and dichloro 1,1′-bis(diphenylphos-phino)ferrocene palladium (II) [$PdCl_2$(dppf)] were purchased from Strem Chemicals. Potassium acetate, carbazole, and potassium carbonate were from Alfa Aesar, Fluka, and Fisher Scientific, respectively. 7,7″-Dibromo-2,2′:7′,2″-ter(9,9-dihexylfluorene) (**5**) was synthesized according to the literature reported [32].

Nuclear magnetic resonance spectra were recorded on a Bruker 400 spectrometer at a resonance frequency of 400 MHz for ^{1}H and 100 MHz for ^{13}C in deuterated solution with a tetramethylsilane (TMS) as a reference for the chemical shifts. Elemental analyses were conducted on a Flash 1112 Series elemental analyzer. The matrix assisted laser desorption ionization time-of-flight mass spectra (MALDI-TOF–MS) of **F1–F4** were measured on a Bruker Autoflex II TOF/TOF mass spectrometer (Bruker Daltonics). Thermogravimetric analysis (TGA) and differential scanning calorimetry (DSC) were carried out using TA instruments TGA-Q500 and DSC-Q100 modules, respectively. The UV–vis absorption and photoluminescence (PL) spectra were recorded on a Shimadzu UV-3101 scanning spectrophotometer and on a Perkin-Elmer LS 55 fluorescence spectrometer, respectively. The absolute PL quantum yields were obtained with a HORIBA-JOBIN-YVON fluoromax-4 spectrofluorometer.

Cyclic voltammetry was performed on a three-electrode AUTOLAB (model PGSTAT30) workstation in deaerated acetonitrile containing ^{n}Bu$_4$NPF$_6$ (0.10 M) as supporting electrolyte at 298 K. A conventional three-electrode cell was used with a platinum working electrode (surface area of 0.3 mm^2) and a gold wire as the counter electrode. The Pt working electrode was routinely polished with polishing alumina suspension and rinsed with acetone before use. The measured potentials were recorded with respect to the Ag/AgCl reference electrode. All electrochemical measurements were carried out under an atmospheric pressure of argon.

The thickness of the film for the OLED device was monitored and calibrated by Dektak 6M Profiler (Veeco). The EL spectra were performed by a JY SPEX CCD3000 spectrometer. Current–voltage–brightness characteristics were measured by using a Keithley 2400 source measurement unit with a calibrated silicon photodiode. All the device testing was carried out in ambient atmosphere.

2.2. Synthesis of 2-bromo-7-(9H-carbazole-9-yl)-9,9-dihexylfluorene (2)

A mixture of 2,7-dibromo-9,9-dihexylfluorene (**1**) (4.923 g, 10.00 mmol), carbazole (1.087 g, 6.50 mmol), copper(I) iodide (124 mg, 0.65 mmol), 1,10-phenanthroline (234 mg, 1.30 mmol) and potassium carbonate (1.973 g, 14.30 mmol) was purged with nitrogen, and then 10 mL of anhydrous DMF was added. The mixture was heated to reflux for 24 h. After cooling to room temperature, the dark suspension was poured into ice-water. The precipitate was collected and purified by silica gel column chromatography eluting with 20:1 hexane/dichloromethane to give **2** as a white solid (2.866 g, 76.2%). ^{1}H NMR ($CDCl_3$, 400 MHz): δ/ppm = 8.18–8.16 (d, 2H, J = 7.6 Hz), 7.89–7.87 (d, 1H, J = 8.0 Hz), 7.64–7.62 (d, 1H, J = 8.8 Hz), 7.55–7.51 (m, 4H), 7.42–7.41 (d, 4H, J = 3.6 Hz), 7.33–7.29 (m, 2H), 2.20–1.96 (m, 4H), 1.16–1.10 (m, 12H), 0.81–0.76 (t, 6H, J = 6.8 Hz), 0.76–0.72 (m, 4H); ^{13}C NMR ($CDCl_3$, 100 MHz): δ/ppm = 153.29, 152.29, 141.07, 139.38, 136.88, 130.27, 126.35, 125.99, 125.95, 123.47, 121.88, 121.48, 121.24, 120.95, 120.40, 119.96, 119.84, 109.75, 55.76, 40.22, 31.51, 29.59, 23.88, 22.54, 13.97; Elemental Analysis (EA): calcd for $C_{37}H_{40}BrN$: C76.80, H6.97, N2.42; found: C76.48, H7.03, N2.67.

2.3. Synthesis of 2-bromo-7-(4-cyanophenyl)-9,9-dihexylfluorene (3)

$Pd(PPh_3)_4$ (37 mg, 3.5% mmol) was added into a mixture of 2,7-dibromo-9,9-dihexylfluorene (**1**) (3.446 g, 7.00 mmol), 4-cyanophenylboronic acid (514 mg, 3.50 mmol) and potassium carbonate (1.693 g, 12.25 mmol) in argon atmosphere. Degassed toluene (35 mL) and water (7 mL) was added into the mixture by a syringe and heated to reflux with continuous stirring in the dark for 24 h under the protection of nitrogen. After cooling to room temperature, the organic layer was separated and the aqueous layer was extracted with ethyl acetate. The combined organic layer was washed with water, brine and dried over sodium sulphate. The solvent was removed under reduced pressure and the crude product was purified by silica gel column chromatography with 5:1 *n*-hexane/ethyl acetate to give **3** as a white powder (1.291 g, 71.6%). ^{1}H NMR ($CDCl_3$, 400 MHz): δ/ppm = 7.76 (s, 1H), 7.75 (s, 4H), 7.60–7.56 (m, 2H), 7.51–7.47 (m, 3H), 2.00–1.96 (m, 4H), 1.14–1.04 (m, 12H), 0.78–0.74 (t, 6H, J = 6.8 Hz), 0.65–0.62 (t, 4H, J = 6.8 Hz); ^{13}C NMR ($CDCl_3$, 100 MHz): δ/ppm = 153.32, 151.46, 145.98, 140.80, 139.32, 138.39, 132.61, 130.22, 127.77, 126.43, 126.34, 121.68, 121.55, 121.38, 120.37, 118.96, 110.83, 55.67, 40.26, 31.45, 29.60, 23.76, 22.54, 13.94. Anal. calcd for $C_{32}H_{36}BrN$: C, 74.70; H, 7.05; N, 2.72. Found: C, 74.32; H, 7.12; N, 3.02.

2.4. Synthesis of 2-(4-cyanophenyl)-7-(4,4,5,5-tetramethyl-1,3,2-dioxaborole-2-yl)-9,9-dihexylfluorene (4)

6 mL degassed dioxane was added into a mixture of **3** (1.028 g, 2.00 mmol), bis(pinacolato)diboron (558 mg, 2.20 mmol), potassium acetate (294 mg, 3.00 mmol), and $PdCl_2$(dppf) (60 mg, 0.06 mmol) with continuously stirring. The mixture was heated at 80 °C for 2 h under nitrogen protection. After cooling to room temperature, the dark suspension was extracted with ethyl acetate and washed with water. The organic layers were combined and dried over sodium sulphate. After the solvent was removed, the crude product was purified by silica gel column chromatography with 5:1 *n*-hexane/ethyl acetate to give **4** as an off-white solid (680 mg, 60.5%). ^{1}H NMR ($CDCl_3$, 400 MHz) δ/ppm = 7.84–7.80 (m, 2H), 7.77–7.72 (m, 6H), 7.58–7.54 (m, 2H), 2.05–1.99 (m, 4H), 1.40 (s, 12H), 1.10–1.03 (m, 12H), 0.76–0.72 (t, 6H, J = 6.8 Hz), 0.63–0.61 (br, 4H). ^{13}C NMR ($CDCl_3$, 100 MHz) δ/ppm = 152.42, 150.27, 146.19, 143.19, 141.75, 138.33, 133.92, 132.58, 128.99, 127.78, 127.74, 126.19, 121.60, 120.68, 119.32, 119.02, 110.71, 83.81, 55.39, 40.21, 31.44, 29.63, 24.07, 23.74, 22.54, 13.95. Elemental Analysis (EA): calcd for $C_{38}H_{48}BNO_2$: C81.27, H8.61, N2.49; found: C81.50, H 8.77, N2.19.

2.5. Synthesis of 7-bromo-7″-(9H-carbazole-9-yl)-2,2′:7′,2″-ter(9,9-dihexylfluorene) (6)

A mixture of 7,7″-dibromo-2,2′:7′,2″-ter(9,9-dihexylfluorene) (**5**) (2.624 g, 2.27 mmol), carbazole (253 mg, 1.51 mmol), copper(I) iodide (29 mg, 0.15 mmol), 1,10-phenanthroline (54 mg, 0.30 mmol) and potassium carbonate (458 mg, 3.32 mmol) was purged with nitrogen, and then 20 mL of anhydrous DMF was added. The mixture was heated to reflux for 24 h. The cooled dark suspension was poured into ice-water to precipitate solid. The solid was collected by filtration and purified by silica gel column chromatography eluting with 50:1 hexane/dichloromethane to give **6** as an off-white solid (952 mg, 50.7%). ^{1}H NMR (CD_2Cl_2, 400 MHz): δ/ppm = 8.22–8.20 (d, J = 7.6 Hz, 2H), 8.02–8.00 (d, J = 8.0 Hz, 1H), 7.93–7.44 (m, 21H), 7.35–7.31 (m, 2H), 2.19–2.05 (m, 12H), 1.17–1.11 (m, 36H), 0.89–0.70 (m, 30H); ^{13}C NMR ($CDCl_3$,

100 MHz): δ/ppm = 153.50, 153.32, 152.92, 151.88, 151.86, 151.85, 151.16, 150.96, 141.18, 141.08, 140.99, 140.45, 140.43, 140.20, 140.14, 140.13, 139.88, 139.55, 139.32, 139.27, 136.41, 130.04, 126.38, 126.31, 126.27, 126.25, 126.22, 125.93, 125.89, 123.45, 121.95, 121.57, 121.51, 121.45, 121.07, 121.01, 120.84, 120.38, 120.16, 120.04, 119.89, 109.85, 55.59, 55.50, 55.40, 40.34, 40.29, 40.24, 31.52, 31.46, 29.66, 29.65, 29.63, 24.00, 23.89, 23.78, 22.56, 22.54, 14.00, 13.99; Elemental Analysis (EA): calcd for $C_{87}H_{104}BrN$: C84.02, H8.43, N1.13; found: C84.01, H8.59, N1.26.

General procedures for Suzuki coupling reaction taking **F1** as an example:

2.6. Synthesis of 2-(9H-carbazole-9-yl)-7-(4-cyanophenyl)-9,9-dihexylfluorene (F1)

$Pd(PPh_3)_4$ (6 mg, 0.6% mmol) was added into a mixture of **2** (289 mg, 0.50 mmol), 4-cyanophenylboronic acid (147 mg, 1.00 mmol) and potassium carbonate (242 mg, 1.75 mmol) in a glove-box. Degassed toluene (5 mL) and water (1 mL) was added into the mixture by a syringe. The mixture was allowed to heat to reflux with continuous stirring in the dark for 24 h under the protection of nitrogen. After cooling to room temperature, the organic layer was separated and the aqueous layer was extracted with ethyl acetate. Organic layers were combined and washed with water, brine and then dried over sodium sulphate. The solvent of the organic solution was removed under reduced pressure and the crude product was purified by silica gel column chromatography with 5:1 *n*-hexane/ethyl acetate to give **F1** as a white powder (205 mg, 68%). ^{1}H NMR (CD_2Cl_2, 400 MHz): δ/ppm = 8.20–8.18 (d, *J* = 7.6 Hz, 2H), 8.01–7.99 (d, *J* = 7.6 Hz, 1H), 7.93–7.91 (d, *J* = 7.6 Hz, 1H), 7.85–7.79 (m, 4H), 7.71–7.68 (m, *J* = 8.0 Hz, 1H), 7.61–7.59 (m, 3H), 7.49–7.43 (m, 4H), 7.34–7.30 (m, 2H), 2.12–2.08 (t, 4H), 1.17–1.12 (br, 12H), 0.80–0.77 (m, 10H); ^{13}C NMR ($CDCl_3$, 100 MHz): δ/ppm = 153.00, 152.14, 146.01, 141.09, 141.07, 139.57, 138.31, 137.00, 132.63, 127.80, 126.51, 126.01, 125.96, 123.50, 121.95, 121.63, 121.21, 120.49, 120.42, 119.99, 118.98, 110.85, 109.77, 55.69, 40.31, 31.51, 29.62, 23.97, 22.53, 13.96; MALDI-TOF–MS: calcd. for $C_{44}H_{44}N_2$: *m*/*z* = 600.35; found: *m*/*z* = 600.32(M^+); Elemental Analysis (EA): calcd for $C_{44}H_{44}N_2$: C87.96, H7.38, N4.66; found: C 87.52, H7.56, N4.92.

2.7. Synthesis of 7-(9H-carbazol-9-yl)-7′-(4-cyanophenyl)-2,2′-bi(9,9-dihexylfluorene) (F2)

Preparation, see the synthesis of **F1**. Batch: **2** (145 mg, 0.25 mmol), **4** (140 mg, 0.25 mmol), potassium carbonate (121 mg, 0.88 mmol), $Pd(PPh_3)_4$ (2 mg, 0.2% mmol). **F2** was obtained as a off-white powder (152 mg, 65.4%). ^{1}H NMR (CD_2Cl_2, 400 MHz): δ/ppm = 8.20–8.18 (d, *J* = 8.0 Hz, 2H), 8.01–7.99 (d, *J* =7.6 Hz, 1H), 7.93–7.58 (m, 15H), 7.49–7.44 (m, 4H), 7.34–7.31 (m, 2H), 2.14–2.12 (br, 8H), 1.15–1.11 (br, 24H), 0.85–0.76 (m, 20H); ^{13}C NMR ($CDCl_3$, 100 MHz): δ/ppm = 152.91, 152.13, 151.94, 151.88, 146.19, 141.59, 141.17, 141.02, 140.79, 140.13, 139.69, 139.59, 137.93, 136.48, 132.61, 127.75, 126.41, 126.39, 126.34, 125.93, 125.91, 123.45, 121.96, 121.59, 120.87, 120.39, 120.35, 120.18, 119.90, 119.03, 110.70, 109.84, 55.60, 55.51, 40.37, 40.33, 31.52, 31.46, 29.65, 23.99, 23.87, 22.54, 13.99, 13.97; MALDI-TOF–MS: calcd. for $C_{69}H_{76}N_2$: *m*/*z* = 932.60; found: *m*/*z* = 932.59 (M^+); Elemental Analysis (EA): calcd for $C_{69}H_{76}N_2$: C88.79, H 8.21, N3.00; found: C88.44, H8.32, N3.24.

2.8. Synthesis of 7-(9H-carbazole-9-yl)-7″-(4-cyanophenyl)-2,2′:7′,2″–ter(9,9-dihexyl-fluorene) (F3)

Preparation, see the synthesis of **F1**. Batch:**6** (380 mg, 0.31 mmol), 4-cyanophenylboronic acid (147 mg, 1.00 mmol), potassium carbonate (150 mg, 1.09 mmol), $Pd(PPh_3)_4$ (3.5 mg, 0.3% mmol). **F3** was obtained as a light yellow powder (258 mg, 63.6%). ^{1}H NMR (CD_2Cl_2, 400 MHz): δ/ppm = 8.21–8.19 (d, *J* = 8.0 Hz, 2H), 8.02–8.00 (d, *J* = 8.0 Hz, 1H), 7.93–7.72 (m, 17H), 7.68–7.66 (m, 2H), 7.62–7.59 (m, 2H), 7.50–7.46 (m, 4H), 7.35–7.33 (m, 2H), 2.16–2.12 (m, 12H), 1.15–1.14 (br, 36H), 0.81–0.78 (m, 30H); ^{13}C NMR ($CDCl_3$, 100 MHz): δ/ppm = 152.92, 152.13, 151.90, 151.88, 151.85, 146.20, 141.63, 141.21, 141.18, 140.98, 140.47, 140.44, 140.20, 140.18, 140.13, 139.56, 139.47, 137.87, 136.42, 132.60, 127.74, 126.39, 126.35, 126.33, 126.27, 125.93, 125.90, 123.45, 121.96, 121.60, 120.84, 120.38, 120.32, 120.16, 120.05, 119.89, 119.04, 110.68, 109.85, 55.59, 55.48, 55.41, 40.37, 31.53, 31.47, 29.67, 29.65, 24.00, 23.90, 23.88, 22.54, 14.00, 13.97; MALDI-TOF–MS: calcd. for $C_{94}H_{108}N_2$: *m*/*z* = 1265.85; found: *m*/*z* = 1265.09 (M^+). Elemental Analysis (EA): calcd for $C_{94}H_{108}N_2$: C89.19, H8.60, N2.21; found: C88.76, H8.77, N2.47.

2.9. Synthesis of 7-(9H-carbazole-9-yl)-7‴-(4-cyanophenyl)-2,2′:7′,2″:7″,2‴-quarter(9,9-dihexylfluorene) (F4)

Preparation, see the synthesis of **F1**. Batch: **6** (312 mg, 0.25 mmol), **4** (140 mg, 0.25 mmol), potassium carbonate (121 mg, 0.88 mmol), $Pd(PPh_3)_4$ (2 mg, 0.2% mmol). **F4** was obtained as a light yellow powder (260 mg, 65.1%). ^{1}H NMR ($CDCl_3$, 400 MHz): δ/ppm = 8.20–8.18 (d, *J* = 8.0 Hz, 2H), 7.97–7.95 (d, *J* = 8.4 Hz, 1H), 7.89–7.58 (m, 27H), 7.49–7.42 (m, 4H), 7.34–7.30 (t, *J* = 7.6 Hz, 2H), 2.12–2.09 (br, 16H), 1.14–1.11 (br, 48H), 0.86–0.76 (br, 40H); ^{13}C–NMR ($CDCl_3$, 100 MHz): δ/ppm = 152.94, 152.15, 151.90, 151.86, 146.22, 141.66, 141.25, 141.20, 141.02, 140.68, 140.64, 140.42, 140.41, 140.39, 140.24, 140.22, 140.21, 140.05, 140.01, 139.55, 139.46, 137.87, 136.42, 132.62, 127.76, 126.39, 126.35, 126.25, 126.23, 125.94, 125.91, 123.46, 121.97, 121.60, 120.85, 120.39, 120.32, 120.16, 120.03, 119.89, 119.05, 110.69, 109.86, 55.61, 55.49, 55.41, 55.40, 40.37, 31.54, 31.47, 29.69, 29.67, 24.01, 23.91, 23.89, 22.55, 14.00, 13.98; MALDI-TOF–MS: calcd for $C_{119}H_{140}N_2$: *m*/*z* = 1598.11; found: *m*/*z* = 1598.49 (M^+). Elemental Analysis (EA): calcd for $C_{119}H_{140}N_2$: C89.42, H8.83, N1.75; found: C88.88, H9.29, N1.83.

2.10. Device fabrication

The solution-processed OLEDs were assembled in a sandwich structure: ITO/PEDOT:PSS/oligomer/TPBi/LiF/Al. The glass substrates covered by indium tin oxide (ITO) were pre-cleaned mechanically with deionized water, methanol, and acetone. A 50 nm-thick layer of poly(ethylenedioxy)thiophene–polystyrenesulphonic acid (PEDOT:PSS) was spin-coated on top of the ITO electrode treated by oxygen plasma. Afterwards, the system was baked at 120 °C for 30 min in a vacuum oven and subsequently moved into a glovebox. A 60 nm-thick emitting layer (**F1**–**F4**) was spin-coated from toluene solution on the PEDOT:PSS layer, followed by being annealed at 120 °C for 30 min to remove residual solvent. TPBi (40 nm), LiF (1 nm), and aluminum (100 nm) were vacuum deposited successively under the pressure $<10^{-4}$ Pa. All the solutions were filtered through 0.22 μm membranes before process. The optimized device of **F4** was fabricated in the configuration of ITO/MoO_3 (8 nm)/NPB (50 nm)/CBP:**F4** (1:4 wt%, 40 nm)/TPBi (25 nm)/LiF (1 nm)/Al (150 nm), in which each layer was thermally deposited under the pressure $<10^{-4}$ Pa. The thicknesses of

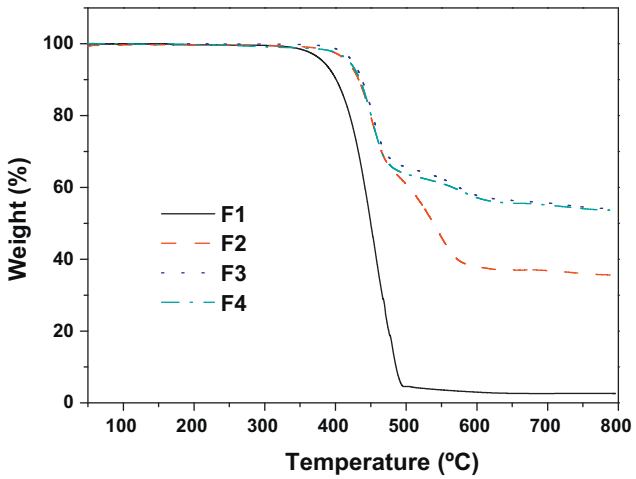

Fig. 1. TGA thermograms of the samples at a heating rate of 10 °C/min measured in dry nitrogen conditions.

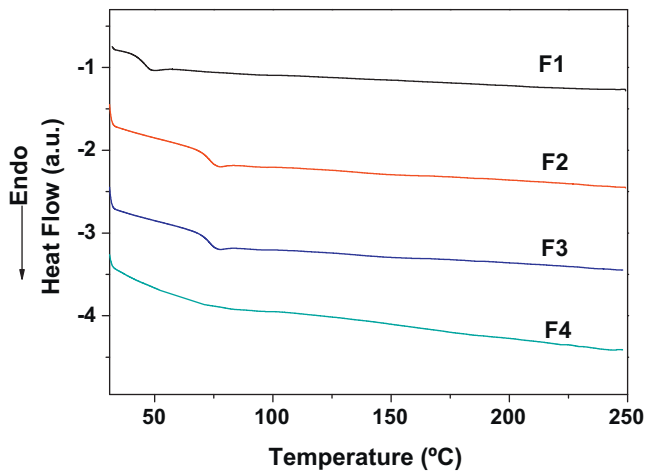

Fig. 2. DSC traces of **F1**, **F2**, **F3**, and **F4** in the second heating process (heating rate: 10 °C/min) measured in dry nitrogen conditions.

the vapor-deposited films were monitored by frequency counter and calibrated by Dektak 6 M Profiler (Veeco), while those of the spin-coated films were controlled by Dektak 6 M Profiler (Veeco) directly. The current density–voltage–luminance characteristics and EL spectra were measured by using a Keithley 2400 source measurement unit with a calibrated silicon photodiode and by a JY SPEX CCD3000 spectrometer, respectively. All the device tests were carried out in ambient atmosphere.

3. Results and discussion

Starting with 2,7-dibromo-9,9-dihexylfluorene (**1**), 2-bromo-7-(9*H*-carbazole-9-yl)-9,9-dihexylfluorene (**2**) and 2-bromo-7-(4-cyanophenyl)-9,9-dihexylfluorene (**3**) were obtained through the Ullmann condensation and Suzuki coupling reaction, respectively. **3** was converted to its corresponding bronic ester **4** when the reaction was catalyzed by $PdCl_2$(dppf). **2** was reacted with 4-cyanophenylboronic acid or **4** to give **F1** or **F2**. 7-Bromo-7″-(9*H*-carbazole-9-yl)-2,2′:7′,2″-ter(9,9-dihexylfluorene) (**6**) was synthesized by the condensation of the dibromo-substituted terfluorene **5** and carbazole. Suzuki coupling reaction of **6** with 4-cyanophenylboronic acid or **4** was employed for the synthesis of **F3** or **F4**, respectively. The molecular structures of the four light-emitting compounds were validated by ^{1}H NMR, ^{13}C NMR, MALDI-TOF–MS (Figs. S1–S3, see supporting information), and elemental analysis (EA). These oligofluorenes are highly soluble in common organic solvents such as toluene, dichloromethane, chloroform, and tetrahedronfuran. Table 1 summarizes the results of MALDI-TOF–MS, TGA, DSC, and photophysical properties of the compounds. TGA and DSC curves are presented in Figs. 1 and 2, respectively. The onset decomposition temperatures (T_d) for the thermal bond cleavage of the oligofluorenes were increased from 352 to 394 °C with increasing number of fluorene units. Besides that, at the end of the heating–up process, the residues of **F1**, **F2**, **F3**, and **F4** were 2.3, 35.5, 54.1, and 53.6 wt%, respectively. This similar trend as that of T_d indicated that the more fluorene units, the better thermal stability could be obtained. The DSC curves of **F1**, **F2**, and **F3** in their second heating cycles showed endothermic baseline shifts at 45, 64, and 70 °C, respectively, at which the glassy states transformed into the supercooled liquid phases (T_g). The DSC trace of **F4** exhibited unconspicuous baseline shift, thereby its T_g was difficult to be identified. In relation to the data reported [12], it could be concluded that in comparison with the cyanophenyl group, the carbazole had better capacity of raising the T_d and T_g values.

The UV/vis absorption and PL spectra of **F1**–**F4** in dilute toluene solutions (~10^{-6} M) and in the thin films are shown in Fig. 3. When measured in solution, the maximum absorptions related to the π–π* transition of the oligomer backbones were in the range of 343–370 nm and increased as the number of the fluorene units. This is due to that more fluorene units resulted in longer conjugated length. It was in great consistent with the carbazole contents that the relative intensity of the shoulder peak at λ = 294 nm, which were originated from the end-capped carbazole units [18,19], decreased orderly from **F1** to **F4**. By using the wavelength of maximum absorption as the excitation wavelength, the PL spectrum of **F1** in dilute toluene solution exhibited a single emission peak at λ = 403 nm, and the other three oligomers showed an emission maximum at 403–410 nm and a shoulder at 422–434 nm. In contrast to the dilute solution absorption spectra, the thin film absorption spectra of **F1**–**F4** displayed a small red-shifts of 2–8 nm due to the weak aggregation effects. The main emission peaks of **F1**, **F2**, and **F3** in thin films were located at 418–420 nm, while the maximum emission of **F4** was shifted to 446 nm with a shoulder peak at 421 nm. This phenomenon was much different from that of the quarterfluorene [11], of which the emission main peak was unchanged in the solid state when compared to that in solution.

Table 1
Physical properties of the series of blue light-emitting oligofluorenes.

Compound	MS	T_d (°C)	T_g (°C)	λ_{abs} [a] (nm)	λ_{em} [a] (nm)	λ_{abs} [b] (nm)	λ_{em} [b] (nm)	Φ_{PL} [c] (%)	Φ_{PL} [d] (%)
F1	600.32	352	45	343 (294)	403	346 (296)	418	97.0	59.2
F2	932.59	383	64	355 (294)	403 (422)	363 (296)	418	97.8	66.7
F3	1265.09	389	70	365 (294)	408 (430)	368 (296)	420 (437)	87.5	66.8
F4	1598.49	394	–	370 (294)	410 (434)	372 (296)	446 (421)	90.5	68.7

[a] Maximum absorption/emission wavelengths in dilute toluene solutions (10^{-6} M).
[b] Maximum absorption/emission wavelengths in the thin films. All the shoulders are shown in the brackets.
[c] Absolute fluorescence quantum yields in dilute toluene solutions.
[d] Absolute fluorescence quantum yields in the thin films.

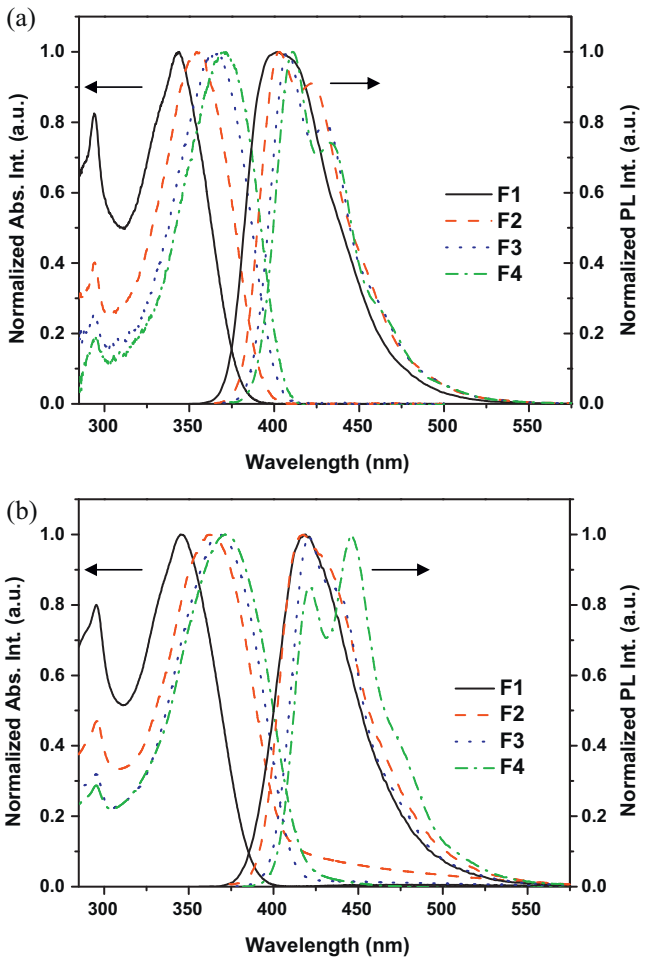

Fig. 3. UV–vis absorption and PL emission spectra ($\lambda_{ex} = \lambda_{abs\_max}$) of **F1–F4** (a) in dilute toluene solution (10^{-6} mol/L) and (b) in the thin films.

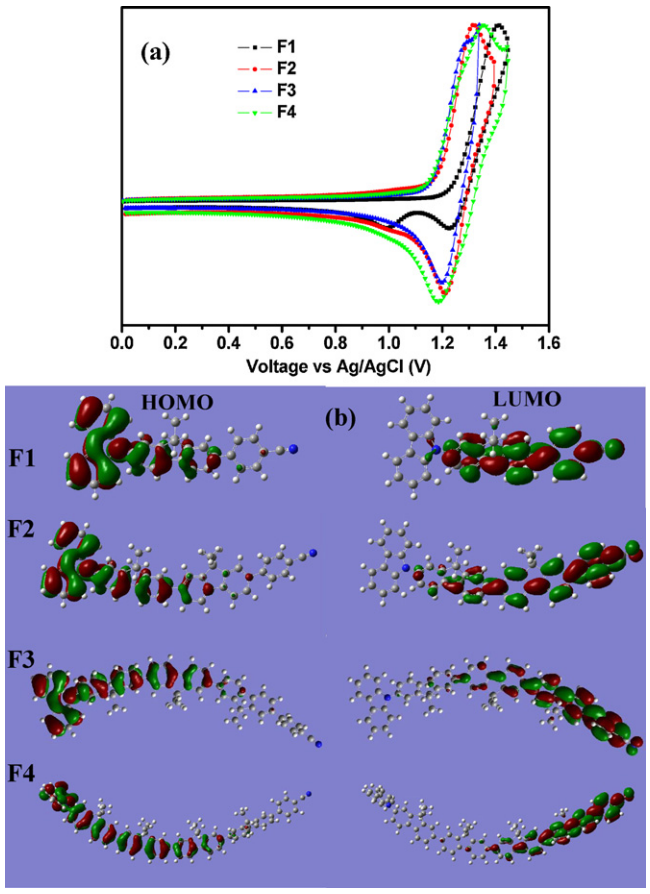

Fig. 4. Cyclic voltammograms of **F1–F4** in 0.1 M $_n$Bu$_4$NPF$_6$ dichloromethane solution at room temperature. Sweep rate 100 mV s^{-1}.

Thus, it could be inferred that the end groups of **F4** led to larger geometry change of the molecule in the solid state, and the electrons in its high singlet excited state were easier to relax to lower singlet excited state. For these reasons, the main emission of **F4** was due to the electron transition from the lower excited state to ground state. By utilizing the HORIBA–JOBIN–YVON instrument, the absolute quantum yields (Φ_{PL}s) of **F1**, **F2**, **F3**, and **F4** in solutions were evaluated as 97.0, 97.8, 87.5, and 90.5%, respectively. The Φ_{PL}s of their thin films drop-casted onto quartz plates were in the range of 59.2–68.7%. These findings indicated that these compounds were excellent fluorescent materials. In the solid state, **F4** possessed the highest quantum yield among these compounds owing to its largest fluorescent fluorene number.

The electrochemical properties of these fluorene-based oligomers were investigated by cyclic voltammetry (CV), as shown in Fig. 4(a). The highest occupied molecular orbital (HOMO) energy levels of the oligomers were calculated from their corresponding onset oxidation potentials according to the equation HOMO $= -(E^{ox}_{onset} + 4.40)$eV with the ferrocene oxidation potential as the standard, where the lowest unoccupied molecular orbital (LUMO) energy levels could be estimated from the corresponding HOMO energy levels and optical band gaps (E_g) [33]. All the compounds showed similar reversible oxidation process in the toluene solution. The onset oxidation potentials of **F1**, **F2**, **F3**, and **F4** were 1.23, 1.18, 1.16, and 1.15 V, respectively. From these data, their HOMO values were estimated to be −5.63, −5.58, −5.56, and −5.55 eV, respectively. By utilizing the equation of LUMO = E_g + HOMO, the LUMO energy levels of **F1**, **F2**, **F3**, and **F4** could be calculated as −2.47, −2.52, −2.53, and −2.55 eV, respectively. When the number of the fluorene units increased, the HOMO energy level rose whereas the LUMO level fell, implying that when the distance between the electron-withdrawing cyanophenyl group and the electron-donating carbazole group extended, the

Table 2
Band gaps and energy levels of the oligofluorenes.

Compound	E_g [a] (eV)	E^{ox}_{onset} [b] (V)	HOMO[c] (eV)	LUMO[d] (eV)	HOMO[e] (eV)	LUMO[e] (eV)	E_g [e] (eV)
F1	3.16	1.23	−5.63	−2.47	−5.38	−1.87	3.51
F2	3.06	1.18	−5.58	−2.52	−5.25	−1.85	3.40
F3	3.03	1.16	−5.56	−2.53	−5.20	−1.85	3.35
F4	3.00	1.15	−5.55	−2.55	−5.17	−1.82	3.35

[a] Determined from UV–vis absorption spectra in toluene solutions.
[b] E^{ox}_{onset}: onset oxidation potential.
[c] HOMO $= -(E^{ox}_{onset} + 4.40)$ eV.
[d] Estimated from HOMO levels and the optical band gaps: LUMO = HOMO + E_g.
[e] Calculated by density-functional theory (DFT) molecular simulation (B3LYP/6-31G(d) level).

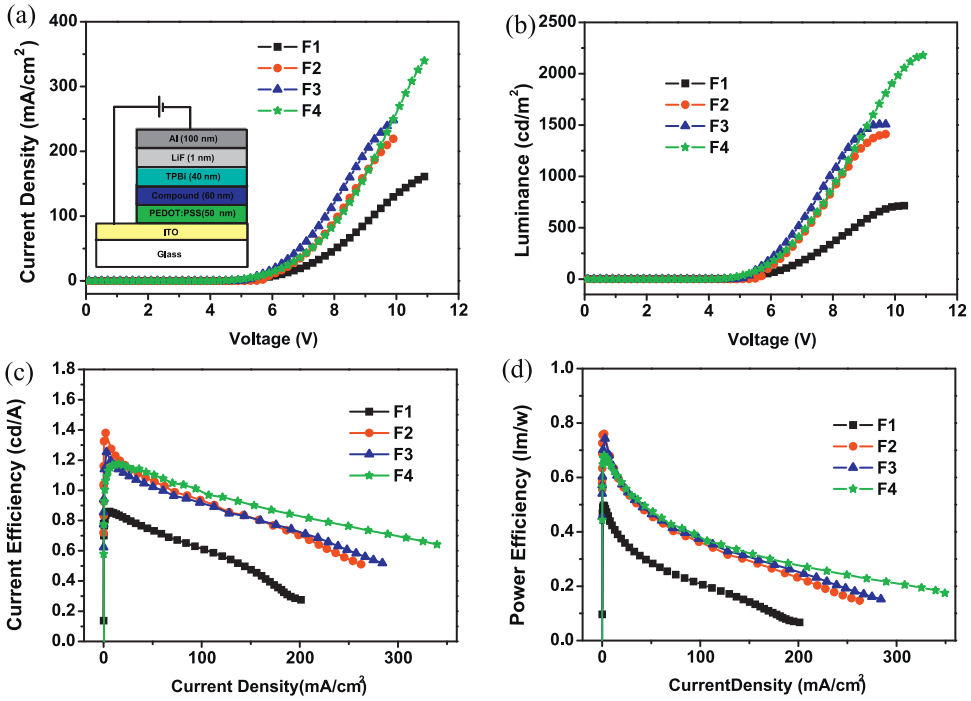

Fig. 5. (a) Current density–voltage (*I–V*), (b) luminance–voltage (*L–V*), (c) current efficiency–current density, and (d) power efficiency–current density characteristics of the ITO/PEDOT:PSS/ETL/TPBi/LiF/Al devices.

molecule was easier to be oxidized or reduced. In other words, the intramolecule interaction caused by the cyanophenyl and carbazole units became less intensive as the amount of the fluorene spacers increased. Moreover, the HOMO and LUMO levels of these cyanophenyl and carbazole end-capped oligofluorenes were lower than those of the carbazole end-capped oligofluorenes [18], suggesting that the hole and electron transporting properties could be effectively modulated through the end groups. To gain insights into the electronic structures, computational studies were carried out on the oligofluorenes using density-functional methods at the B3LYP/6-31G(d) level, as shown in Fig. 4(b). For each oligomer, the majority of the electron distribution of the HOMO was found to be located over the carbazole and neighboring fluorene entities; whereas the electron distribution of the

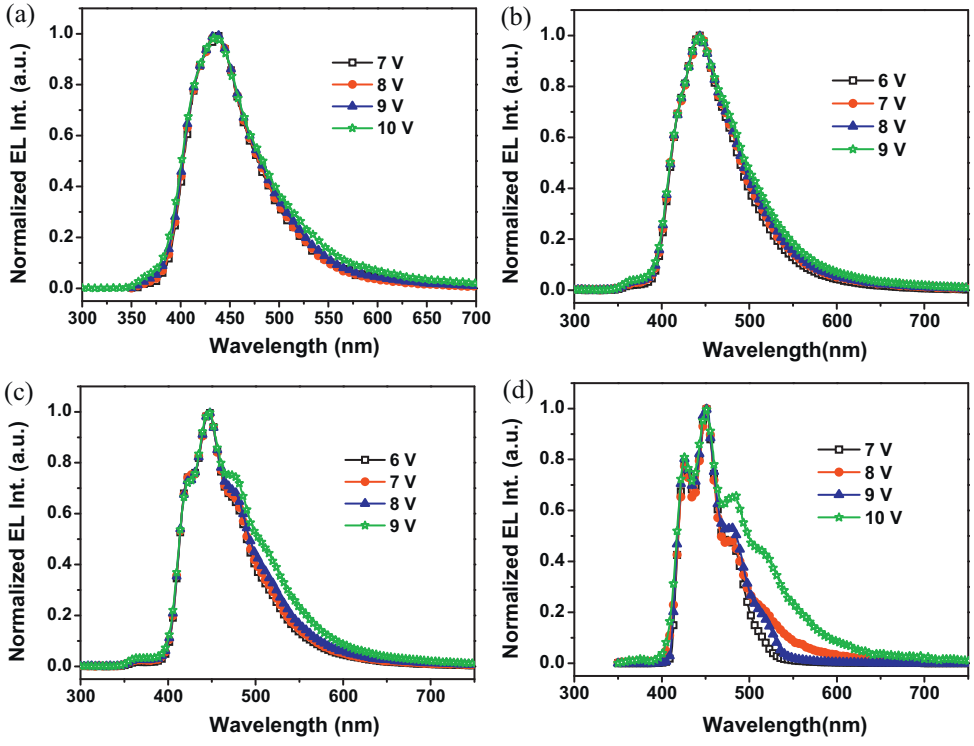

Fig. 6. EL spectra of (a) **F1**, (b) **F2**, (c) **F3**, (d) **F4** recorded at different applied voltages with the device configuration of ITO/PEDOT:PSS/ETL/TPBi/LiF/Al.

Table 3
EL performance of the devices based on the series of blue light-emitting oligofluorenes.

Emissive layer	$V_{turn\text{-}on}$ [c] (V)	L_{max} [d] (cd/m^2)	$V_{L,max}$ [e] (V)	η_c@100 cd/m^2 [f] (cd/A)	η_c@1000 cd/m [g] (cd/A)	$\eta_{c,max}$ [h] (cd/A)	$\eta_{p,max}$ [i] (lm/w)	λ_{EL} [j] (nm)	CIE1931 [k] (x, y)
F1[a]	4.7	714	10.3	0.84	–	0.86	0.50	437	(0.17, 0.12)
F2[a]	5.1	1410	9.7	1.28	0.90	1.38	0.76	443	(0.18, 0.19)
F3[a]	4.7	1507	9.7	1.19	0.89	1.25	0.74	446 (423, 475)	(0.18, 0.19)
F4[a]	4.1	2180	10.9	1.17	0.97	1.17	0.68	450 (426, 481)	(0.18, 0.20)
CBP/F4[b]	6.9	5135	15.3	1.70	1.42	1.76	0.85	416 (442)	(0.16, 0.09)

[a] These results were obtained with the device configuration of ITO/PEDOT:PSS/ETL/TPBi/LiF/Al.
[b] The device structure was ITO/MoO_3/NPB/CBP:**F4**(1:4)/TPBi/LiF/Al.
[c] Turn-on voltage corresponding to 1 cd/m^2 of luminance.
[d] Maximum luminance.
[e] Driving voltage corresponding to maximum luminance.
[f] Current efficiency at the luminance of 100 cd/m^2.
[g] Current efficiency at the luminance of 1000 cd/m^2.
[h] Maximum current efficiency.
[i] Maximum power efficiency.
[j] Maximum EL wavelength.
[k] CIE coordinates measured at the $V_{L,max}$.

LUMO was located mainly over the cyanophenylfluorene entities. As summarized in Table 2, the calculated results, including the HOMO, LUMO, and HOMO–LUMO gaps, were all slightly higher than the corresponding electrochemically measured values. The calculated HOMO levels of **F1**, **F2**, **F3**, and **F4** were −5.38, −5.25, −5.20, and −5.17 eV, respectively. The increase of the conjugation length elevates the HOMO energy levels of the parent oligomer, but has no large effect to the LUMO levels. The molecular simulation results show that the carbazole end-groups serve as electron donors and the cyanophenyl terminals as electron acceptors.

To investigate the electroluminescence (EL) properties of the oligomers, the OLED devices were fabricated using the configuration of ITO/PEDOT:PSS(50 nm)/compound(60 nm)/TPBi(40 nm)/LiF (1 nm)/Al(100 nm). Poly(ethylenedioxy)thiophene mixed with poly(styrene sulphonic acid) (PEDOT:PSS) was used as the hole injection layer. 1,3,5-Tris(1-phenyl-1H-benzimidazol -2-yl)benzene (TPBi) and LiF were introduced as electron transporting and injection layers, respectively. As shown in Fig. 5, the device based on **F4** displayed the lowest turn-on voltage (4.1 V) and highest maximum luminance (2180 cd/m^2) among the devices. The highest luminances of **F1**, **F2**, and **F3** were 714, 1410, and 1507 cd/m^2, respectively. These results indicated that the amount of the fluorescent fluorene units had direct relation with the brightness. When **F2** and **F3**-based devices displayed maximum brightness, their operating voltage were both 9.7 V, whereas, for the **F1** and **F4**-based devices, the voltages were 10.3 and 10.9 V, respectively. Thereby, the EL spectra of these devices would not be recorded in the same range of voltages (Fig. 6). The current efficiencies (η_cs) of the devices were calculated by the equation of $\eta_c = L/(10I)$, in which L was the luminance, and I was the corresponding current density at the same voltage. Although the maximum η_c of **F4** (1.17 cd/A) was not as high as that of **F2** (1.38 cd/A), the curve of **F4** decayed slowest, even at the brightness of 1000 cd/m^2. The current efficiency value of the **F4**-based device was 0.97 cd/A, while the values of **F2** and **F3** were 0.90 and 0.89 cd/A, respectively. The maximum power efficiencies (η_ps) of

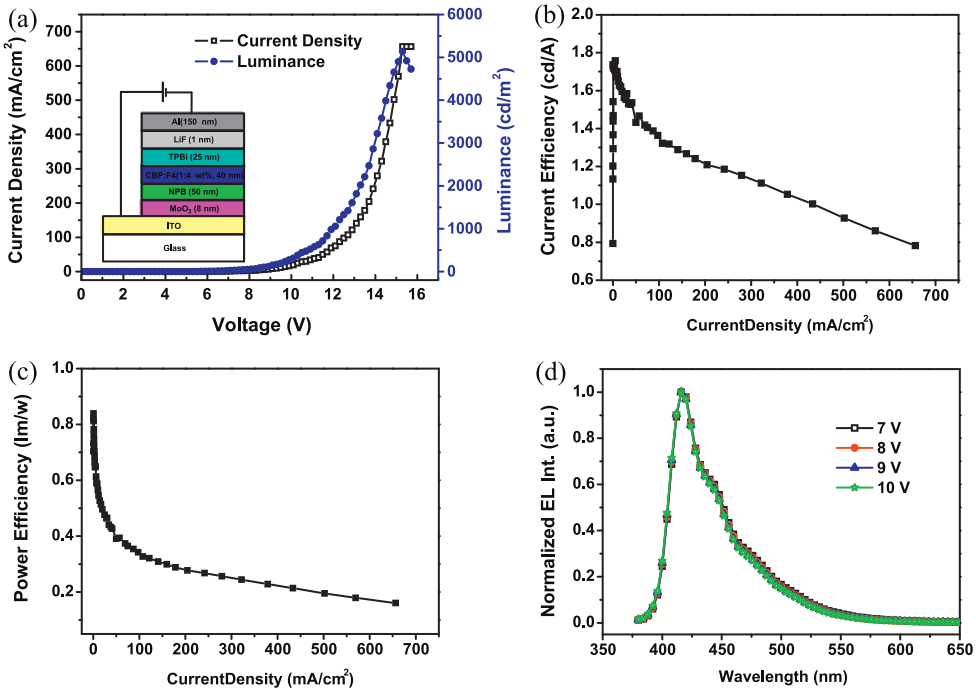

Fig. 7. (a) Current density–voltage–luminance (I–V–L) characteristics, (b) current efficiency–current density relationship, (c) plots of power efficiency–current density, and (d) normalized EL spectra recorded from 7 to 10 V of the ITO/MoO_3/NPB/CBP:**F4**(1:4)/TPBi/LiF/Al device.

these compounds were found to be in the range of 0.50–0.76 lm/w, and still, the decline of **F4** was the gentlest. All the devices emitted deep blue light when they were operating. It was worthy to note that the EL curves of **F1** and **F2** were almost voltage-independent but those of **F3** and **F4** had larger change when driven at higher voltages. This could be explained as follows: for **F1** and **F2**, the molecular chains were short and the end groups hindered the π–π stacking effect under electric field. When the intensity of the electric field increased, **F3** and **F4**, in which the end groups might have weak aggregation-suppressing function to the longer molecular chains, were easy to rearrange and aggregate into cluster, therefore the long-wavelength EL emission was intensified. When these devices were operated at their corresponding $V_{L,max}$ (see Table 3), the CIE coordinates (x, y) of **F1**, **F2**, **F3**, and **F4** were (0.17, 0.12), (0.18, 0.19), (0.18, 0.19), and (0.18, 0.20), respectively. All the CIE coordinates were in the blue region of the CIE 1931 diagram.

We have known that **F4** was the brightest oligofluorene among the four blue light-emitting compounds. To further improve its device performance, we fabricated the doped device of ITO/MoO_3(8 nm)/NPB(50 nm)/CBP:**F4**(1:4 wt%, 40 nm)/TPBi(25 nm)/LiF (1 nm)/Al(150 nm) using vapor deposition method. MoO_3 and 4,4′-bis[*N*-(1-naphthyl)-*N*-phenylamino]biphenyl (NPB) were used as hole injection and transporting layers, respectively. In the emitting layer, 25 wt% of 4,4′-N,N′-dicarbazole-biphenyl (CBP) was doped into **F4**. The device performance results were shown in Fig. 7. Compared with the undoped device based on **F4**, the turn-on voltage of the doped device was raised to 6.9 V, which might be caused by the hole-blocking effect of CBP [34]. The doped device exhibited maximum luminance of 5135 cd/m^2, operating voltage tolerance from 6.9 to 15.3 V, highest current efficiency ($\eta_{c.max}$) of 1.76 cd/A, and power efficiency ($\eta_{p.max}$) of 0.85 lm/w, respectively. The improved device performance might be resulted from the increased purity and morphology via the deposition method and the increase of the exciton formation in the emitting layer due to the hole-confining capacity of CBP. In addition, the EL spectra of the CBP:**F4** device were voltage-independent, indicating that the existence of CBP could effectively inhibit the rearrangement and aggregation of the **F4** molecules under electric field. The CIE coordinates (x, y) of this device was (0.16, 0.09), which located at the deep blue area of CIE 1931 diagram.

4. Conclusion

We have successfully synthesized four oligofluorene-based push–pull type blue light-emitting functional materials and investigated their thermal, photophysical, electrochemical, and electroluminescent properties. The onset decomposition temperatures for the thermal bond cleavage were increased from 352 to 394 °C with increasing molecular weights of the light-emitting compounds. The DSC curves of **F1**, **F2**, and **F3** in the second heating cycles showed T_g at 45, 64, and 70 °C, respectively, whereas the T_g of **F4** was difficult to be determined. In dilute toluene solution, these oligofluorenes exhibited main absorption peaks in the range of 343–370 nm, photoluminescence maxima from 403 to 410 nm, and absolute quantum yields (Φ_{PL}) of higher than 87%. The absorption spectra of these compounds in thin films had no large differences from those in the solutions except for the small red-shifts (2–8 nm) caused by the weak aggregation effects. The main PL emission maxima of **F1**, **F2**, and **F3** in thin films were located at 418–420 nm. But for **F4**, the maximum emission was shifted to 446 nm and the peak at 421 nm became shoulder. This is because the cyanophenyl and carbazole end groups complicated its energy levels, and the electrons in the high singlet excited state were easier to relax to lower singlet excited state, thereby the main emission energy was lower. The absolute Φ_{PL}s of the oligofluorenes measured in thin films were estimated in the range of 59.2–68.7%. By using CV measurements together with the optical band gaps in solutions, the HOMO(LUMO) energy values of **F1**, **F2**, **F3**, and **F4** were estimated to be −5.63(−2.47), −5.58(−2.52), −5.56(−2.53), and −5.55(−2.55) eV, respectively. The device based on solution-processed **F4** displayed the lowest turn-on voltage (4.1 V) and highest maximum luminance (2180 cd/m^2) with maximal current efficiency of 1.17 cd/A among those based on the oligofluorenes in the configuration of ITO/PEDOT:PSS/oligofluorenes/TPBi/LiF/Al. When the intensity of the electric field increased, **F3** and **F4** with longer molecular chain with end-groups were easy to rearrange and aggregate, therefore their EL spectra were voltage-dependent. With the vapor-deposited device of ITO/MoO_3/NPB/CBP:**F4**(1:4)/TPBi/LiF/Al, improved device performance and voltage-independent EL spectra with the CIE coordinates of (0.16, 0.09) were obtained.

Acknowledgements

The authors are grateful for the financial support of the National Natural Science Foundation of China (21074034), Ministry of Education of China (309013), the Fundamental Research Funds for the Central Universities, Shanghai Municipal Educational Commission for the Shuguang fellowship (08GG10, to Y.C.) and the Shanghai Eastern Scholarship (to Y.C.).

Appendix A. Supplementary data

Supplementary data associated with this article can be found, in the online version, at doi:10.1016/j.jphotochem.2011.12.008.

References

[1] M. Gross, D.C. Muller, H.G. Nothofer, U. Sherf, D. Neher, C. Brauchle, K. Meerholz, Improving the performance of doped π-conjugated polymers for use in organic light-emitting diodes, Nature 405 (2000) 661–665.
[2] J.M. Hancock, A.P. Gifford, Y. Zhu, Y. Lou, S.A. Jenekhe, n-Type conjugated oligoquinoline and oligoquinoxaline with triphenylamine endgroups: efficient ambipolar light emitters for device applications, Chem. Mater. 18 (2006) 4924–4932.
[3] P.L. Burn, S.C. Lo, I.D.W. Samuel, The development of light-emitting dendrimers for displays, Adv. Mater. 19 (2007) 1675–1688.
[4] L. Schmidt-Mende, A. Fechtenkötter, K. Müllen, E. Moons, R.H. Friend, J.D. MacKenzie, Self-organized discotic liquid crystals for high-efficiency organic photovoltaics, Science 293 (2001) 1119–1122.
[5] M.S. Wong, Z.H. Li, Y. Tao, M. D'Iorio, Synthesis and functional properties of donor–acceptor π-conjugated oligomers, Chem. Mater. 15 (2003) 1198–1203.
[6] F. Lincker, N. Delbosc, S. Bailly, R. De Bettignies, M. Billon, A. Pron, R. Demadrille, Fluorenone-based molecules for bulk-heterojunction solar cells: synthesis, characterization, and photovoltaic properties, Adv. Funct. Mater. 18 (2008) 3444–3453.
[7] H. Meng, J. Zheng, A.J. Lovinger, B.C. Wang, P.G. Van Patten, Z.N. Bao, Oligofluorene–thiophene derivatives as high-performance semiconductors for organic thin film transistors, Chem. Mater. 15 (2003) 1778–1787.
[8] A. Facchetti, M. Mushrush, M.H. Yoon, G.R. Hutchison, M.A. Ratner, T.J. Marks, Building blocks for n-type molecular and polymeric electronics. Perfluoroalkyl- versus alkyl-functionalized oligothiophenes (*n*T; n = 2–6). Systematics of thin film microstructure, semiconductor performance, and modeling of majority charge injection in field-effect transistors, J. Am. Chem. Soc. 126 (2004) 13859–13874.
[9] R.P. Ortiz, J. Casado, V. Hernandez, J.T.L. Navarrete, J.A. Letizia, M.A. Ratner, A. Facchetti, T.J. Marks, Thiophene–diazine molecular semiconductors: synthesis, structural, electrochemical, optical, and electronic structural properties; implementation in organic field-effect transistors, Chem. Eur. J. 15 (2009) 5023–5039.
[10] C. Poriel, J.J. Liang, J. Rault-Berthelot, F. Barrière, N. Cocherel, A.M.Z. Slawin, D. Horhant, M. Virboul, G. Alcaraz, N. Audebrand, L. Vignau, N. Huby, G. Wantz, L. Hirsch, Dispirofluorene–indenofluorene derivatives as new building blocks for blue organic electroluminescent devices and electroactive polymers, Chem. Eur. J. 13 (2007) 10055–10069.
[11] L.S. Chinelatto Jr., J. del Barrio, M. Pinol, L. Oriola, M.A. Matranga, M.P. De Santob, R. Barberi, Oligofluorene blue emitters for cholesteric liquid crystal lasers, J. Photochem. Photobiol. A: Chem. 210 (2010) 130–139.
[12] A.C. Grimsdale, K.L. Chan, R.E. Martin, P.G. Jokisz, A.B. Holmes, Synthesis of light-emitting conjugated polymers for applications in electroluminescent devices, Chem. Rev. 109 (2009) 897–1091.

[13] S. Tao, Z.K. Peng, X.H. Zhang, P.F. Wang, C.S. Lee, S.T. Lee, Highly efficient non-doped blue organic light-emitting diodes based on fluorene derivatives with high thermal stability, Adv. Func. Mater. 15 (2005) 1716–1721.
[14] S.H. Lee, T. Tsutsui, Molecular design of fluorene-based polymers and oligomers for organic light-emitting diodes, Thin Solid Films 363 (2000) 76–80.
[15] S. Tang, M.R. Liu, C. Gu, Y. Zhao, P. Lu, D. Lu, L.L. Liu, F.Z. Shen, B. Yang, Y.G. Ma, Synthesis and electrochemical properties of peripheral carbazole functional ter(9,9-spirobifluorene)s, J. Org. Chem. 73 (2008) 4212–4218.
[16] Q.G. Kong, D. Zhu, Y.W. Quan, Q.M. Chen, J.F. Ding, J.P. Lu, Y. Tao, Multi-H shaped macrocyclic oligomers consisting of triphenylamine and oligofluorene: synthesis and optoelectronic properties, Chem. Mater. 19 (2007) 3309–3318.
[17] Q.D. Liu, J.P. Lu, J.F. Ding, M. Day, Y. Tao, P. Barrios, J. Stupak, K. Chan, J.J. Li, Y. Chi, Monodisperse starburst oligofluorene-functionalized 4 4′,4″-tris(carbazol-9-yl)-triphenylamines: their synthesis and deep-blue fluorescence properties for organic light-emitting diode applications, Adv. Funct. Mater. 17 (2007) 1028–1036.
[18] V. Promarak, S. Saengsuwan, S. Jungsuttiwong, T. Sudyoadsuk, T. Keawin, Synthesis and characterization of N-carbazole end-capped oligofluorenes, Tetrahedron Lett. 48 (2007) 89–93.
[19] V. Promarak, A. Punkvuang, T. Sudyoadsuk, S. Jungsuttiwong, S. Saengsuwan, T. Keawin, K. Sirithip, Synthesis and characterization of N-carbazole end-capped oligofluorene–thiophenes, Tetrahedron 63 (2007) 8881–8890.
[20] M.S. Liu, X.Z. Jiang, P. Herguth, A.K.Y. Jen, Efficient cyano-containing electron-transporting polymers for light-emitting diodes, Chem. Mater. 13 (2001) 3820–3822.
[21] M.S. Liu, X.Z. Jiang, S. Liu, P. Herguth, A.K.Y. Jen, Effect of cyano substituents on electron affinity and electron-transporting properties of conjugated polymers, Macromolecules 35 (2002) 3532–3538.
[22] Y. Lin, Z.K. Chen, T.L. Te, Y.F. Dai, D.G. Ma, Z. Ma, Q.D. Liu, Y. Chen, Conjugated copolymers comprised of cyanophenyl substituted spirobifluorene and tricarbazole–triphenylamine repeat units for blue light-emitting diodes, J. Polym. Sci. Part A: Polym. Chem. 48 (2010) 292–301.
[23] Y. Lin, Z.K. Chen, T.L. Ye, Y.F. Dai, D.G. Ma, Z. Ma, Q.D. Liu, Y. Chen, Novel fluorene-based light-emitting copolymers containing cyanophenyl pendants and carbazole-triphenylamines: synthesis, characterization and their PLED application, Polymer 51 (2010) 1270–1278.
[24] C.F Shu, R. Dodda, F.I. Wu, M.S. Liu, A.K.Y. Jen, Highly efficient blue-light-emitting diodes from polyfluorene containing bipolar pendant groups, Macromolecules 36 (2003) 6698–6703.
[25] F.I. Wu, D.S. Reddy, C.F. Shu, M.S. Liu, A.K.Y. Jen, Novel oxadiazole-containing polyfluorene with efficient blue electroluminescence, Chem. Mater. 15 (2003) 269–274.
[26] X.W. Zhan, Y.Q. Liu, X. Wu, S. Wang, D.B. Zhu, New series of blue-emitting and electron-transporting copolymers based on fluorene, Macromolecules 35 (2002) 2529–2537.
[27] Y. Lin, Y. Chen, Z.K. Chen, D.G. Ma, B. Zhang, T.L. Ye, Y.F. Dai, Triphenylamine and quinoline-containing polyfluorene for blue light-emitting diodes, Eur. Polym. J. 46 (2010) 997–1003.
[28] H.J. Jiang, H.Y. Wang, R. Zhu, J.H. Wan, F. Liu, J.C. Feng, W. Wei, W. Huang, Two novel oligomers based on fluorene and pyridine: correlation between the structures and optoelectronic properties, J. Polym. Sci. Part A: Polym. Chem. 46 (2008) 1548–1558.
[29] S.J. Su, T. Chiba, T. Takeda, J. Kido, Pyridine-containing triphenylbenzene derivatives with high electron mobility for highly efficient phosphorescent OLEDs, Adv. Mater. 20 (2008) 2125–2130.
[30] J.H. Park, N.S. Cho, Y.K. Jung, H.J. Cho, H.K. Shim, H. Kim, Y.S. Lee, Polymeric light emitting properties and structural relationships of fluorene-based conjugated copolymers containing various hole transporting derivatives, Org. Electron. 8 (2007) 272–285.
[31] C.G. Zhen, Z.K. Chen, Q.D. Liu, Y.F. Dai, R.Y.C. Shin, S.Y. Chang, J. Kieffer, Fluorene-based oligomers for highly efficient and stable organic blue-light-emitting diodes, Adv. Mater. 21 (2009) 2425–2429.
[32] H.S. Yang, W.F. Xie, Y. Zhao, J.Y. Hou, S.Y. Liu, Enhanced current efficiency in organic light-emitting devices using 4,4′-N N′-dicarbazole-biphenyl as hole-buffer layer, Solid-State Electron. 51 (2007) 111–114.
[33] Y.N. Li, J.F. Ding, M. Day, Y. Tao, J.P. Lu, M. D'iorio, Novel stable blue-light-emitting oligofluorene networks immobilized by boronic acid anhydride linkage, Chem. Mater. 15 (2003) 4936–4943.
[34] Q. Zhang, J.S. Chen, Y.X. Cheng, L.X. Wang, D.G. Ma, X.B. Jing, F.S. Wang, Novel hole-transporting materials based on 1,4-bis(carbazolyl)benzene for organic light-emitting devices, J. Mater. Chem. 14 (2004) 895–900.